

Ship Collision Events Against Reinforced Concrete Offshore Structures

L. Márquez & P. Rigo

University of Liège, Liège, Belgium

H. Le Sourne

GeM Institute, ICAM, Nantes, France

ABSTRACT: The number of Floating Offshore Wind Turbines (FOWT) is expected to increase significantly in the coming years to face the challenges of the current global decarbonization policies. The use of materials such as Reinforced Concrete in the floating substructures becomes then attractive for reducing both maintenance and chain manufacturing costs, as seen in different industrial scale prototypes such as Floatgen from BW-IDEOL. The non-linear behavior of plain concrete, in addition to numerical complications related to explicit reinforcement modeling, makes the elastic-plastic calculations of these structural elements particularly challenging. In this work, a numerical study of different constitutive concrete models available in the commercial software LS-DYNA is presented, whose capabilities in modeling flexural and shear failure arising from ship collisions events are tested using structural elements with geometrical and mechanical properties similar to those found in current FOWT prototypes.

1 INTRODUCTION

In recent years, the number of operational Floating Offshore Wind Turbines (FOWT) prototypes has been increasing as this technology is reaching a high level of industrial readiness, whereas in designs such as Floatgen from BW-IDEOL the floating substructure is made entirely of Reinforced Concrete (RC) - see Fig. (1). The introduction of these structures, which present relatively low thicknesses in comparison with Offshore RC structures used in the past for the Oil & Gas (O&G) industry, requires special attention regarding accidental events such as ship collisions with both service and commercial ships, as the structure needs to dissipate a significant part of the collision energy while preserving its watertightness. Minimizing then the risk of flooding between compartments becomes a priority.

Ship collision events with steel offshore structures have been studied deeply for different kinds of platforms (e.g., Monopiles, Jackets, Floating), leading to comprehensive design standards to account for accidental loads due to ship impacts as the DNV-RP-C204 (2019). Usually, the analysis of collision events is based on simplified empirical models as proposed by Minorsky (1958), Non-Linear Finite Element Analysis (NL-FEA) as carried out by Le Sourne et al. (2015) and Storheim et al. (2014), or formulations based on external dynamics along with structural dissipation mechanisms which are normally build using rigid plastic analysis, as shown in the work of Zhang

(1999) and Buldgen et al. (2014). However, the research involving ship collision against RC structures is limited, especially in the case of Offshore Wind Turbines.

In the work of Furnes et al. (1980), the complications and consequences of collisions between supply ships and reinforced concrete walls with similar geometrical and mechanical properties to those found in O&G offshore platforms were addressed. It was pointed out that offshore shell structures with thicknesses above 0.5 m were not prone to suffer high damage levels as their stiffness was significantly higher than the studied ship hulls, while the most critical failure to be checked was punching shear. Additionally, supply vessels with displacements of 2500 Ton with velocities between 0.5 - 2 m/s were found not a threat for these structures.

More recently, a numerical analysis of ship collisions against prestressed RC pontoon walls was carried out by Sha et al. (2019), where a dynamic punching shear check method was proposed. Moreover, the concrete, reinforcement bars, and tendons of a 0.9 m RC wall were explicitly modeled and integrated into the collision analysis using NL-FE in which the effects of tendon prestress, wall thickness, and ship bulb geometries were studied. In this work, it was not only observed that prestressing improved the shear capacity of the wall, but also the high sensitivity of the structural damage with respect to the relative strength between the ship and the collided structure.

Despite the previously mentioned research, the work regarding collision events against offshore RC structures is scarce, a consequence of the highly rigid structures used in the past combined with the limitations of the available concrete constitutive models in NL-FEA.

Currently, classification societies guidelines for FOWT structural design such as DNV-GL-ST-0119 (2018) emphasize on a better assessment of the loads arising from collision events in comparison with fixed substructures, as the implications of compartment penetration are more critical. Additionally, they require that the analysis of concrete structures needs to account for the local and global behavior of the impacted structure, as well as for its post-damage integrity as expressed in DNV-GL-ST-502 (2019), which assumes collisions with Offshore Supply Vessels (OSV) with displacements no less than 5000 Ton and velocities of 0.5 m/s for Ultimate Limit State (ULS) verification. However, the accuracy of the current concrete constitutive models available in NL-FEA has not been assessed properly for these events.

The use of NL-FEA involving accidental loading of RC structures has been largely explored in high-velocity events such a blast loading and aircraft impacts as presented in Daudeville et al. (2011), applications for which pressure-dependent elastic-plastic models describing the nonlinear behavior of concrete have been developed and proved to lead to accurate results, as seen in the work of Broadhouse (1995) and Wu et al. (2015). Some of these models have proven to be useful in medium velocity impact scenarios like car collisions with bridge columns, application for which a concrete material was created by the U.S department of transportation -see Murray (2007), while some of them have been used in low-velocity events such as barge collisions against bridge piers -see Sha et al. (2013). Nevertheless, these material models have not been studied for the relatively low thicknesses and stress states found in ship-FOWT collision events. It is the objective then of the present work to test the capabilities of some of the most used concrete material models available in the commercial software LS-DYNA regarding ship collision events.

2 CONCRETE MATERIAL MODELS

Concrete is a porous and granular material widely used in structural applications such as buildings, bridges, nuclear plants, offshore structures, etc. The compressive uniaxial behavior of this material is nonlinear from the very beginning of the load application and is directly influenced by the mixture characteristics and its drying time. For characterizing the behavior of plain concrete, uniaxial compression tests along different confinement pressures are required, as the hydrostatic pressure increases the ultimate load that



Figure 1. Floatgen FOWT Reinforced Concrete substructure. Courtesy of BW-IDEOL.

the material can withstand, contrary to what occurs in materials such as steel.

Ideally, a constitutive model for plain concrete should be able to capture shear dilation, compressive pre-peak hardening, post-peak softening, stiffness degradation, confinement effects on the strength and strain rate effects while including an accurate cracking formulation for capturing both local (shear) and global damage (flexural) at the structural level.

Different concrete models including these properties have been developed for quasi-static, blast and impact loads. However, most of them require several parameters to properly model the entire behavior of the concrete yield surface. On the other hand, some of these models have been built in such a way that few parameters (e.g., aggregate size, tangent modulus, compressive strength) are required for building their failure surfaces, reducing this way experimental efforts and costs. These models, which are explored in the present work, have in common an isotropic Hooke's law-based elastic update before yield, differing only in the way of calculating their yield surfaces and stiffness degradation during the plastic update, whose parameters are calibrated based on experimental data for a given application and concrete characteristics. Consequently, high uncertainties arises when modeling different structural stress states from the ones that they were made for. The choice of any constitutive model will depend then on a proper understanding of its limitations for a given stress state.

2.1 Winfrith Concrete Model (WM)

This material model was developed by Broadhouse (1995) to supply the needs of the Nuclear industry to study accidental impact events. The plasticity formulation of this model is based on the shear failure surface proposed by Ottosen as shown in Eq. (1),

$$F(I_1, J_2, \cos 3\theta) = a \frac{J_2}{f_c^2} + \gamma \frac{\sqrt{J_2}}{f_c} + b \frac{I_1}{f_c} - 1 \quad (1)$$

Where I_1 is the first invariant of the stress tensor, J_2 the second invariant of the deviatoric stress tensor, Θ the Lode angle and a , b and γ the parameters that control the shape of the failure surface, which are extracted experimentally for different Compressive-Tensile strength f_c/f_t ratios as discussed in Schwer (2010). On the other hand, the crack modeling is based on the specific fracture energy G_{tf} required to form a tensile crack in a brittle material, which is equal to the work required to propagate a crack in a given surface.

$$w = A \frac{G_{tf}}{f_t} \quad (2)$$

The crack width w is given then by Eq. (2), where A is the coefficient of proportionality of the area enclosed by the curve. The values of the fracture energy depend on f_t and the aggregate size, which are implemented in this model according to the recommendations of the CEB (1990) and calibrated with respect to the element size, this way avoiding mesh dependency. Although the WM can model explicit cracking through the element (i.e., crack width), no damage degradation is implemented. Instead, an elastic-perfectly plastic behavior is observed in compression while softening based on G_{tf} is used in tension failure. On the other hand, the strain rate effects are accounted in compression by the Dynamic Amplification Factors (DIF) recommended by CEB (1990) and applied to the Young, shear, and bulk moduli, as well as the compressive and tensile strengths. In the work of Wu et al. (2012) was pointed out that this model does not account for shear dilation nor compressive post-peak softening. Additionally, when tested at the structural level in RC structures subjected to blast loading and high-velocity impact, the response was overly stiff, most probably due to its inability to model compressive post-peak softening. The same behavior was also observed when used in impact against RC beams, as shown in the work of Saini et al. (2019).

2.2 Karagozian & Case Concrete Model (KCC)

The KCC was developed initially for modeling RC structures submitted to blast loadings and through the years has been modified to account for quasi-static and impact loads. The plasticity formulation of this model is based on three pressure-dependent strength surfaces named yield strength surface σ_y , maximum strength surface σ_m and residual strength surface σ_r , along a damage parameter λ which is function of the effective plastic strain ε_{ep} . The plasticity yield function depends then on J_2 , the dynamic failure surface Γ that is interpolated from the strength surfaces, the current damage parameter λ and an associativity parameter ω as:

$$F(I_1, J_2, J_3, \lambda) = \sqrt{3J_2} - \omega\Gamma(I_1, J_3, \lambda) \quad (3)$$

$$\sigma_i(p) = a_{0i} + \frac{p}{a_{1i} + a_{2i}p} \quad (4)$$

Where a_{ni} are the strength surface parameters with $i=m, y, r$ and which are determined by scaling the inputted f_c with known experimental values carried out by the developers in normal-weight concrete with a generic f_c of 45.4 MPa as expressed in Wu et al. (2015).

The damage evolution parameter λ is built for both tension and compression states and it is mesh regularized according to localization width and fracture energy test data based on the CEB (1990), while the associativity parameter ω accounts for the volume expansion effects, whose dependence on the element size in high confinement states becomes relevant. As in the WM, the strain rate effects are accounted for using the recommendations by CEB (1990) in compression, while for tension a modified formulation is used to avoid duplications of inertial effects as discussed in Magallanes et al. (2010). However, only the compressive strengths and damage parameters are modified when these effects are accounted for.

A series of single elements simulations in the work of Wu et al. (2012) showed that the material can model shear dilation, pre-peak hardening, post-peak softening while capturing very well the strength enhancement with confinement effects. At the structural level, it behaved quite well in blast loading and high-velocity impact applications. However, the model presented instabilities when used without strain rate effects, even in quasi-static applications, which is also observed in the works of Wu et al. (2015) and Saini et al. (2019).

2.3 Continuous Surface Cap Model (CSCM)

This constitutive model was developed by the U.S department of transportation to be used in road safety applications, targeting normal strength concretes (between 28 and 58 MPa) under low confinement. Its yield function is composed of a shear failure surface F_s , a hardening cap F_c to include the plastic volume changes related to pore collapse, and a Rubin scaling function \mathfrak{R} that modifies the shape of the yield function to include the effects of the third invariant of the deviatoric tensor J_3 , avoiding this way to model the same strength for torsion and both triaxial tension and compression – see Murray (2007).

$$F(I_1, J_2, J_3) = J_2 - \mathfrak{R}^2 F_S^2 F_C \quad (5)$$

All the parameters required for building the strength surfaces are obtained by data fitting within the range of concretes previously mentioned. The damage formulation of this material is based on a damage

parameter d which degrades the stress tensor directly in the visco-plasticity algorithm, as well as the shear G and bulk moduli K as shown in Eq. (7). Damage is distinguished between brittle and ductile respectively, the latter accumulated due to compressive pressure while the former due to tensile pressure. In the same way as the previous models, the mesh regularization is based on keeping constant the tensile fracture energy G_{tf} for a given element size using the relation given by the CEB (1990) as shown in Eq. (6), which relates the fracture energy with the compressive strength and the maximum aggregate size.

$$G_{tf} = G_{F0} \left(\frac{f_c}{10}\right)^{0.7} \quad (6)$$

$$E^{damaged} = (1 - d)E^{undamaged} \quad (7)$$

Where G_{F0} is the fracture energy at $f_c = 10$ MPa and function of the maximum aggregate size. The values for the compressive and shear fracture energies are settled in $100G_{tf}$ and $1G_{tf}$ respectively. The strain rate effects are included in the form of a two-parameter visco-plastic formulation, whose values are calibrated from DIF's coming from in-house data, as it is claimed that better fitting is obtained compared to the CEB (1990). These effects are accounted for in both strength and damage parameters.

As the KCC, this model behaved quite well in the single element simulations as well as in triaxial compression tests made on cylinders performed in the works of Wu et al. (2012) and Saini et al. (2019), leading only to inaccurate results when using high confinement pressures. At the structural level for high-velocity applications, the model led to accurate results in both works, while for quasistatic and blasting loads behaved either too compliant, or too stiff. In the case of low-velocity impacts against RC beams as shown in Saini et al. (2019), this model presented little dependence on hourglass coefficients.

3 RIGID IMPACT ON RC SLABS

Before testing the capabilities of the previously mentioned models in RC slabs subjected ship collisions, one of the experimental tests carried out by Hrynyk et al. (2014) was recreated numerically, as experimental data for ship collisions against RC FOWT or similar structures are not available in the literature. Although the stress states of these slabs are not the same as the ones found in ship collision analysis, they are more similar than the existent works on blast loading applications or RC beams impact.

Single element simulations in uniaxial compression were performed to compare the stress-strain behavior of the material models with different element sizes. A f_c of 69.4 MPa was used along with an aggregate size of 13 mm to automatically generate the

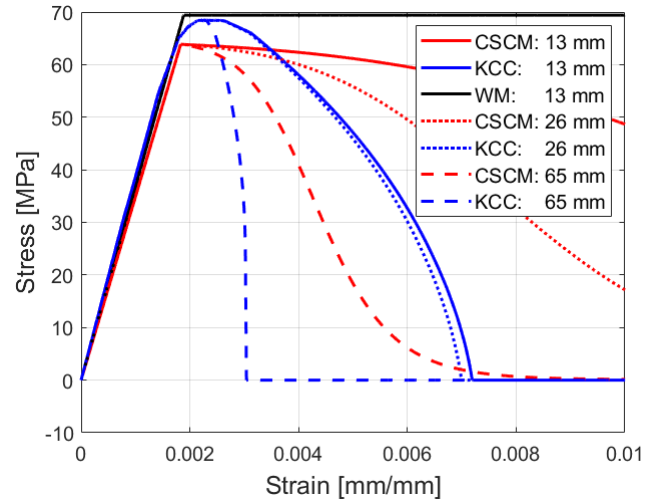


Figure 2. Single element simulations for different element sizes.

concrete material parameters as in the test TH2-1 by Hrynyk et al. (2014). In Fig. (2) can be observed that for the CSCM and KCC materials, the larger the element size, the sooner the failure, consequence of both models mesh regularization: regardless the element size, the elements fail at its respective compressive fracture energy G_{cf} , while the same elastic-perfectly plastic behavior of the WM is observed independently of the element size. Moreover, for a given element size, the fracture energy in the KCC seems to be the lowest of all the models, from which we can expect sooner failure in the case of unconfined compressive stress states.

From the drop weight tests carried out by Hrynyk et al. (2014), the test TH2-1 was selected as no fiber nor shear reinforcement was present in the specimen. In this test, a mass of 150 Kg with a squared impact face was dropped from a height of 3.26 m, equivalently having an initial impact velocity of 8 m/s. Additionally, the supports allowed the corners of the slab to rotate, but both vertical and horizontal displacements were restricted. The transversal displacement was recorded using a series of potentiometers and crack contours were presented for each test.

A numerical model of this experiment was built in LS-DYNA where the concrete, reinforcements bars and contact supports were modeled explicitly using the slab specimen properties as shown in Fig. (3) and Table. (1). A rigid material with an equivalent mass

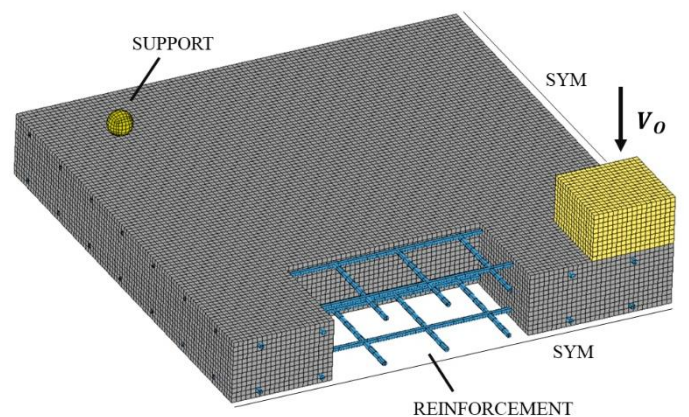


Figure 3. Numerical model of the Hrynyk TH2 Specimen.

was used to build the impactor, while the concrete was modeled using under integrated 8 node solid hexahedrons along with a constant stress formulation. The reinforcements were modeled using beam elements with Hughes-Liu formulation and were coupled to the concrete elements using a constraint-based coupling along the normal direction with two coupling points per beam element. Moreover, a stiffness form of the Flanagan-Belytschko hourglass control for solids was used.

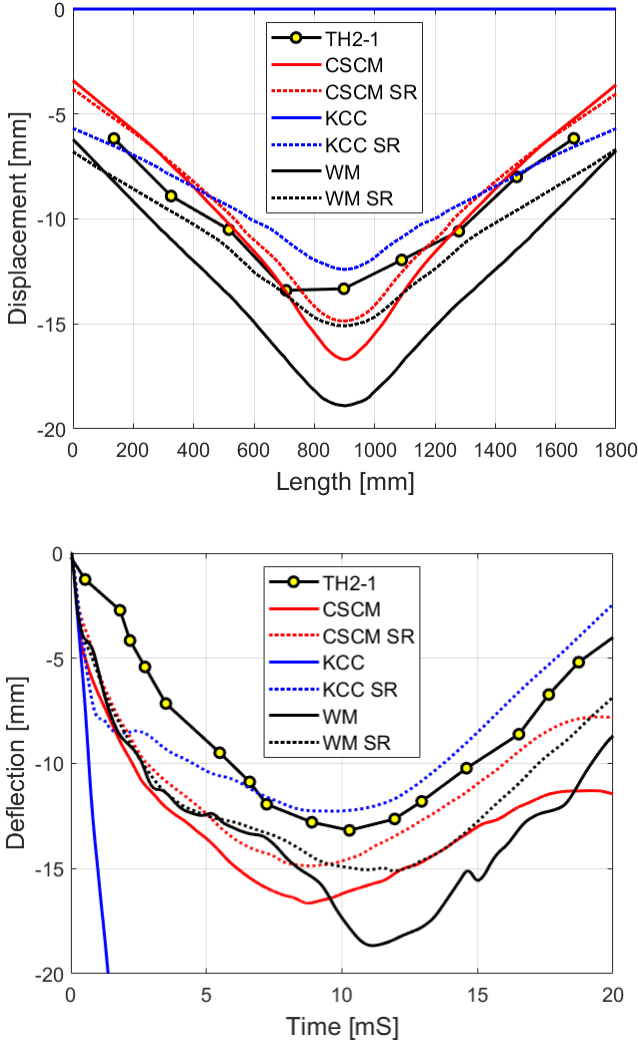


Figure 5. Displacement profile at maximum deflection (Top) and central deflection time history (Bottom).

Table 1. Hrynyk TH2-1 and FOWT slab parameters.

Parameters	Hrynyk	FOWT	Units
Impactor Weight	0.15	2000	Ton
Slab Width and Height	1800	9000	mm
Slab Thickness	130	300	mm
Compressive Strength f_c	69.4	42	MPa
Aggregate size	13	10	mm
Rebar Diameter	9.5	20	mm
Rebar Spacing	130	150	mm
Clear cover	16	30	mm
Rebar f_y [MPa]	489	420	MPa
Rebar E [GPa]	193	205	GPa
P^*	5	5	[-]
C^*	40.4	40.4	s^{-1}

* Used in numerical simulations with SR effects.

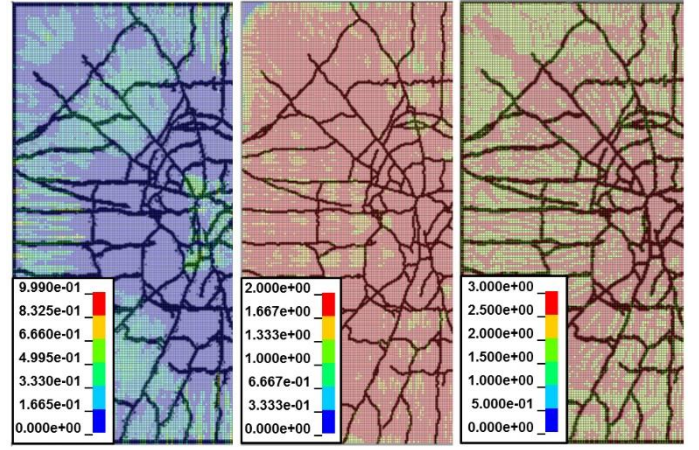


Figure 4. Experimental crack contours (black lines) placed over the different material damage contours at maximum displacement. From left to right: CSCM, KCC and WM.

The results of the numerical simulations of the three different concrete constitutive materials are summarized in Fig. (4). An element size of 10 mm for both concrete and rebar elements was used after carrying out a mesh sensitivity analysis where all the material models converged in terms of central displacement and slab internal energy. Moreover, a comparison between the models considering the strain rate effects for both concrete and steel was performed, the latter being included by the Cowper-Symonds formulation with the material parameters P and C shown in Table. (1).

In terms of the impact response period and displacement profile at maximum displacement, all the material models except the KCC and WM without strain rates presented a good agreement with the experimental results, thus remarking the influence of the strain rate effect consideration for this specific problem. However, the KCC model was highly unstable when the strain rate effects were not included, even when the initial velocity impact was reduced, a problem experienced also in the works of Wu et al. (2012) and Saini et al. (2019). Regarding the maximum midpoint displacement, all the material models presented an error of less than 14% when the strain rates were active, being the most accurate the KCC and CSCM models. It is important to remark that additional numerical instabilities were present in the KCC numerical simulations, especially at the beginning of the impact when the shockwave dissipation was taking place. Although treatment of the material bulk viscosity improved the problems, they were not eliminated. Moreover, this material was highly affected by the hourglass formulation and its coefficient values, which did not occur with the CSCM and WM materials.

On the other hand, in the Fig. (5) are presented the damage contours of the materials for the maximum midpoint deflection. The CSCM and WM present a good correlation in capturing a great part of the experimental crack pattern, the former underestimating the damage around the central zone and the latter

capturing the damage spreading through the corners; in contrast, the KCC highly overestimated the damage along the entire RC slab. Nevertheless, the analysis of damage patterns for the present material models needs to be done cautiously: although they provide good insights into how the RC slab is damaging through the impact, they do not lead always to trustable results. Moreover, different researchers have used different concrete erosion criteria based on principal strains, effective plastic strain, or shear strains to better describe the crack pattern of the RC members. However, there is still no consensus about which of these criteria better describe the concrete erosion, which comes with additional numerical complications such as non-conservation of energy or early failure triggering in surrounding elements.

4 SHIP COLLISIONS

When studying ship collision events against floating RC structures, the quantification of the energy transfer should consider not only the coupling between the external dynamics and internal mechanics of the collided bodies, but also the different failure mechanisms found at the structural level such as shear punching. In the assessment of Accidental Limit States (ALS), design guidelines such as DNV-GL-ST-0119 (2018) recommend considering impact loads with the maximum authorized vessel along speeds no less than 2 m/s. As the aim of the present work is not to check whether the current FOWT RC structures can sustain the accidental design loads, but rather to see the capabilities of the aforementioned concrete materials in ship collision analysis, low impact energy cases are tested to avoid this way compartment penetration or large element deformations. In this study, a rigid bulb of a typical Offshore Supply (OSV) with 2000 Tons of displacement is impacted against a fully clamped squared isotropically reinforced RC slab with similar characteristics to the ones used in Floatgen from BW-IDEOL, which was simplified in the current work for both confidential and practical reasons.

The FOWT motions in this study are disregarded as the displacement ratio between the FOWT and ship is more than four, and no shear reinforcement nor pre-tensioned tendons are considered: although both effects can significantly influence the resistance of the RC slab, they would increase the numerical complexity of the current problem and the comparison of the concrete constitutive models may be obscured by additional uncertainties (i.e., prestressing and hydro coupling subroutines). Similarly, a rigid bulb was assumed in order to avoid complexities regarding the large deformation of the bulb structure, leaving this way the RC slab as the only structure able to dissipate impact energy. Although these assumptions lead to conservative results in terms of structural

deformation, they allow to compare the different constitutive models directly. The impactor and material properties are summarized in the Fig. (6) and Table. (1), where the concrete failure parameters were automatically generated for the given f_c and aggregate size.

The same concrete and rebar element types used in the previous control simulations were considered to model the FOWT RC slab, as well as the same hour-glass control subroutine. A mesh convergence analysis was performed for all constitutive models where good convergence in terms of force-displacement curves and internal energy absorption was observed, except for the KCC material model, for which extremely compliant behaviors were observed through all the simulations. An element size of 30 mm was found to be the best compromise in accuracy and computational effort, which led to a ratio of 10 elements through the slab thickness, similar to the one used in the previous control simulations. In Fig. (8) are shown the displacement profiles at maximum deflection and the force-displacement curve for the WM and CSCM materials with and without strain rate effects. A combination of both flexural and shear response is observed in both materials, although none of them failed completely though the thickness as shown in Fig. (7). Both WM and CSCM materials led to similar results in terms of maximum deflection profile; however, a very compliant behavior was observed in the WM when including strain rate effects,

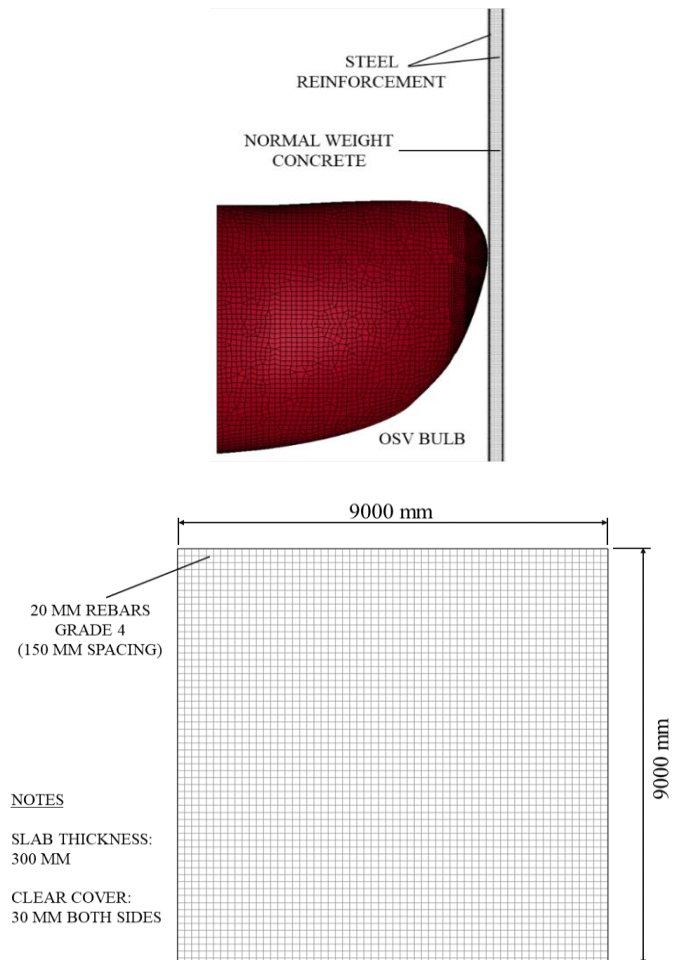


Figure 6. Collision scheme and RC slab geometrical characteristics.

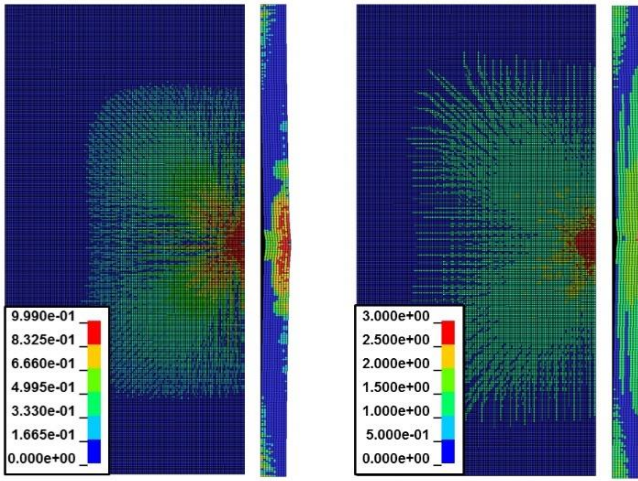


Figure 7. Damage contours at max deflection: CSCM (Left) and WM (Right)

an unphysical behavior that had been previously reported in works such as Wu et al. (2013). When observing the force-displacement curves in Fig. (8), it is seen that the WM led to a stiffer solution than the CSCM, which was more than expected due to the incapability of this material to account for post-peak softening. Regarding the damage contours, both materials led to similar results as presented in Fig. (7), whose difference relied mainly upon the extension of the damage through-thickness, being more localized in the case of the CSCM. On the other hand, all the simulations using the KCC led to extremely compliant results, even for impact energies smaller than 0.09 MJ, as severe damage was propagated through almost all the slab elements from the early collision phase. Different numerical treatments such as variation of hourglass control subroutines, bulk viscosity control, and variation of the associativity parameter ω were tried without success, as the material presented always an extremely fragile and compliant behavior.

Several impact energies up to 10 MJ were also tested varying the ship initial velocity, except for the case of 10 MJ, in which a ship displacement of 5000 Ton with an impact velocity of 2 m/s was used. The force-displacement curves without strain rate effects are presented in Fig. (9). For the 0.09 MJ and 1 MJ impact scenarios, it was observed that punching was not developed completely through the thickness, leading then to a combined flexural and a localized deformation at the impact point. In contrast, for impact energies above 4 MJ, several damages through the cross-section were observed in addition to reinforcement failure, which led to penetration of the compartment. Moreover, the inertial effects for the higher impact energies can be observed in the early phase of the force-displacement curves, where the early slab stiffness is higher compared to the low energy cases. For impacts above 4 MJ, a resistance plateau of almost 5 MN is consistent in both material models, although this is sustained entirely by the reinforcement contribution as a punching cone is already formed in the RC slab.

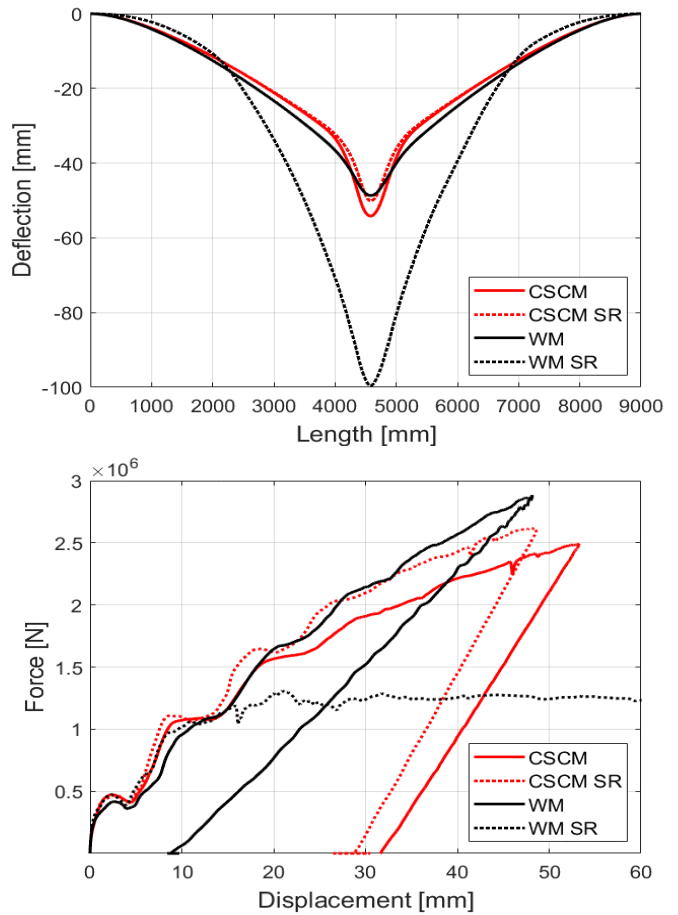


Figure 7. Displacement profile at maximum deflection (Top) and Force-Displacement curves for an impact energy of 0.09 MJ (Bottom).

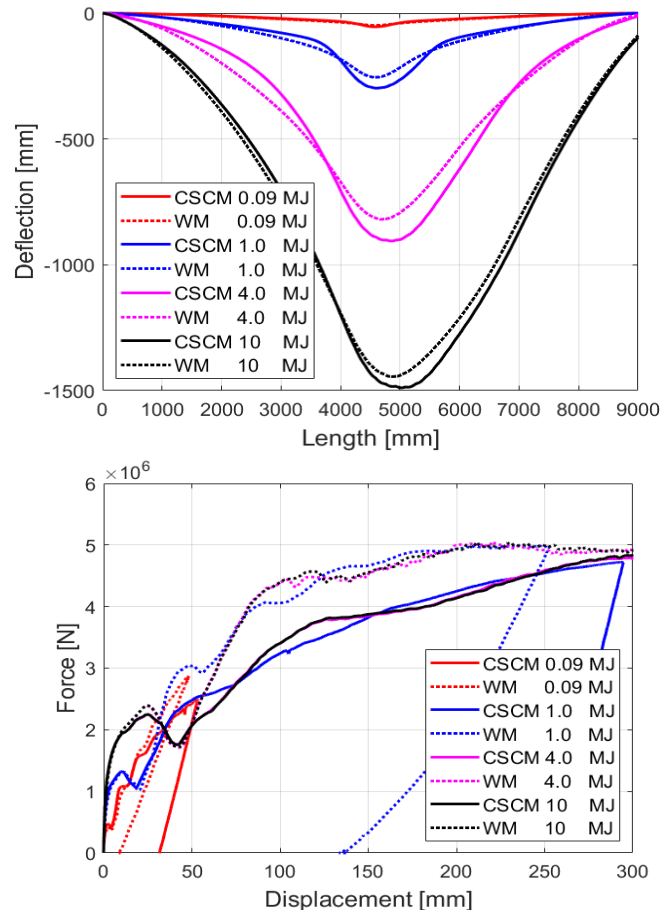


Figure 9. Displacement profile at maximum deflection (Top) and Force-Displacement curves (Bottom) for different impact energies.

5 CONCLUSIONS

A series of control simulations at both element and structural scale were carried out to test the capabilities of some of the concrete constitutive models available in LS-DYNA, especially in stress states similar to those found in ship collisions against FOWT's. Their correspondent yield surfaces and damage parameters were automatically generated based on their concrete compressive strength and aggregate size.

The single element simulations corroborated that the fracture energy is maintained constant regardless the element size. On the other hand, the Hrynyk control simulation at structural level revealed some discrepancies between the constitutive models in terms of structural stiffness, although all the material models were able to provide a solution within a 14 % error margin in terms of maximum displacement. In the case of the KCC material, a non-physical behavior was observed when the strain rate effects were not considered, in addition to high dependency on the hourglass formulations and their coefficients.

In the ship collision simulations, good agreement was observed between the CSCM and WM models along the different impact energies: both models captured similar force-displacement curves, and the damage contours agreed well between each other. However, the WM produced stiffer solutions, which was expected due to the model post-peak elastic-perfectly plastic behavior. In contrast, the KCC model could not produce meaningful results in the studied ship collision cases, as almost all the elements were highly damaged from the very beginning of the impact, even for small impact energies.

From this work, it transpires that the current simplified input concrete material models can produce meaningful and consistent results in ship collision events. However, the lack of experimental research up to this day does not allow to draw any conclusion about the accuracy of the results. Moreover, the present limitations of the constitutive models should be accounted accordingly to the collision scenario: The CSCM cannot handle high confinement pressures, the WM model is not able to model post-peak softening nor accurate strain rate effects, and the KCC presents several numerical instabilities for the studied energies. Therefore, further numerical and experimental research is recommended for assessing the accuracy and capabilities of these materials regarding ship collisions against FOWT's.

6 ACKNOWLEDGMENTS

The authors would like to thank the Fonds de la Recherche Scientifique (FNRS) for their support under the funding grant FRIA, and IDEOL for their technical support. Part of this work was performed within the framework of WEAMEC, West Atlantic Marine

Energy Community, granted by ICAM Engineering School, Pays de la Loire Region and Europe (European Regional Development Fund) and within COLFLOWT project from the Walloon Region (Plan Marshall- GreenWin-Belgium) 2021-2023.

7 REFERENCES

- Broadhouse, B.J. 1995. The Winfrith Concrete Model in LS-DYNA3D. In AEA Technology report.
- Buldgen, L., Le Sourne, H. & Pire, T. 2014. Extension of the super-elements method to the analysis of a jacket impacted by a ship. In *Marine structures* 38(2014) 44-71.
- CEB. 1990. CEB-FIP Model code 90. Federation Internationale de la Precontrainte.
- Daudeville, L. & Malécot, Y. 2011. Concrete structures under impact. In *European Journal of Environmental and Civil Engineering* 15(SI), 2011, 101-140.
- DNV-GL, RP-C204. 2019. Structural design against accidental loads. Edition 2019-09.
- DNV-GL, ST-0119. 2018. Floating wind turbine structures. Edition 2018-07.
- DNV-GL, ST-502. 2019. Offshore concrete structures. Edition 2018-02.
- Furnes, O. & Amdahl, J. 1980. Ship collisions with offshore platforms.
- Hrynyk, T. & Vecchio, F. 2014. Behavior of steel fiber reinforced concrete slabs under impact load. In *ACI structural journal* V.111, No.5.
- Le Sourne, H., Barrera, A. & Maliakel, J.B. 2015. Numerical crashworthiness analysis of an offshore wind turbine jacket impacted by a ship. In *Journal of Marine Science and Technology* Vol.23, No.5, pp 694-704.
- Magallanes, J.M., Wu, Y., Malvar, J. & Crawford, J.E. 2010. Recent improvements to release III of the K&C concrete model. In 11th int. LS-DYNA users conf. proceedings.
- Minorsky, V. 1958. An analysis of ship collisions with reference to protection of nuclear power plants. New York: Sharp (George G.).
- Murray, Y.D. 2007. Users manual for LS-DYNA concrete material model 159. FHWA-HRT-05-062.
- Saini, D. & Shafei, B. 2019. Concrete constitutive models for low velocity impact simulations. In *Int. Journal of Impact Engineering* 132(2019) 103329.
- Schwer, L. 2010. An introduction to the Winfrith concrete model. In report of Schwer Engineering & Consulting services.
- Sha, Y. & Hao, H. 2013. Laboratory tests and numerical simulations of barge impact on circular reinforced concrete piers. In *Engineering structures* 46(2013) 593-605.
- Sha, Y. & Amdahl, J. 2019. Numerical investigations of a prestressed pontoon wall subjected to ship collision loads. In *Ocean Engineering* 172(2019) 234-244.
- Storheim, M. & Amdahl, J. 2014. Design of offshore structures against accidental ship collisions. In *Marine Structures* 37(2014) 135-172.
- Wu, Y., Crawford, J.E. & Magallanes, J.M. 2012. Performance of LS-DYNA concrete constitutive models. In 12th int. LS-DYNA users conf. proceedings.
- Wu, Y., Crawford, J.E., Lan, S. & Magallanes, J.M. 2013. Validation studies for concrete constitutive models with blast test data. In 13th int. LS-DYNA users conf. proceedings.
- Wu, Y. & Crawford, J.E. 2015. Numerical modeling of concrete using a partially associative plasticity model. In *Journal of Engineering Mechanics ASCE*.
- Zhang, S. 1999. The mechanics of ship collisions. Technical University of Denmark PhD thesis.